2022

Three-Dimensional Modeling of the Solidification Front in Ice Cubes

Guilherme M. Berno

Fernando Knabben

Christian Hermes

Three-Dimensional Modeling of the Solidification Front in Ice Cubes

Guilherme M. BERNO, Fernando T. KNABBEN, Christian J. L. HERMES *

POLO Laboratories, Department of Mechanical Engineering, Federal University of Santa Catarina
Florianópolis, SC, Brazil

* Corresponding Author: hermes@polo.ufsc.br

ABSTRACT

Ice makers are no longer a high-end feature but a must in modern domestic refrigerators. In order to maximize the ice production rate without compromising the refrigerator performance, the solidification of water must be analyzed in the most realistic fashion. In this context, the present work is aimed at putting forward a three-dimensional moving-boundary model to calculate the water solidification in ice trays subjected to operating conditions typically found in household appliances. To better understand the physical phenomena and validate the model, experiments were performed in a purpose-built closed-loop wind-tunnel facility at -23 °C and air flow rate of 10 $m^3 h^{-1}$ using a single volume of 145 ml fed with distilled, mineral, and filtered tap water. The end of the solidification process was identified by monitoring the cooling curves with the aid of seven thermocouples placed within the ice cube. In the numerical front, the ice cube was modeled as a pyramid trunk and Stefan's formulation was applied to each of the domain boundaries so that the ice thickness could be calculated over time. Deviations within a ±10% error band were observed for all cases. A good agreement between the model predictions for the time evolution of the ice cube temperature and the experimental counterparts was also verified. In addition, literature data for the position of the solidification front and the remaining liquid fraction were fairly predicted by the model.

1. INTRODUCTION

In household refrigerators, automatic ice machines, also known as icemakers, cyclically fill a storage reservoir that can be placed within the freezer compartment or the refrigerator door. In general, icemakers are cooled by forced convection using the cold air from the freezer. The ice production starts by feeding water into a tray. Then the water is cooled down and freezes, so that the formed ice can be harvested. The icemaking cycle is then restarted, and the processes are repeated until the ice bucket is loaded.

During the ice production, the intense heat transfer can negatively affect the temperature of the other compartments of the refrigerator. Literature results showed that the mean temperature changes in the refrigerator compartments when the icemaker is turned on with no change in thermostat settings (Yashar and Park, 2011; Meier and Martinez, 1996). According to the US Department of Energy (DOE), refrigerators with an embedded icemaker consume more energy than those without it (Yashar, 2012). As stated by Yashar and Park (2011) icemakers can add up to 20% to the annual consumption of the appliance. Thus, the use of mathematical models to predict the freezing time and ice production rate can significantly contribute to improving the performance of refrigerators equipped with icemakers.

However, the mathematical modeling of the icemaking process is not trivial. The phase change problem is highly non-linear and exact solutions exist only for simpler one-dimensional scenarios, as is the case of the analytical expressions proposed by Plank (1913) and Plank (1941) for the freezing time, based on the pioneering study of Stefan (1891). For most applications, it is necessary to use numerical models, which not only take into account the convection in the liquid, of great importance in the heat transfer between phases and in the evolution of the liquid/solid interface (Morgan, 1981; Voller and Prakash, 1987), but also allow the simulation of multidimensional geometries subjected to realistic initial and boundary conditions.

Numerical methods for phase change can be divided into two main categories: variable and fixed mesh (Samarskii *et al.*, 1993). Variable mesh methods must somehow equate the position of the interface and, for this reason, are also

called interface location methods. In this case, the discrete phase change interface is continuously tracked, and the mesh is transformed or deformed to adapt to this interface. Another approach is to vary the time interval so that the boundary coincides with the existing mesh lines at each step of the solution, but this method is hardly applied to multidimensional cases (Hu *et al.*, 1996). Unlike a moving mesh method, the fixed mesh ones identify the solidification front *a posteriori* with the solution of the temperature field or other marking variable. Fixed mesh methods are considered simpler, mainly from an implementation standpoint (Voller *et al.*, 1990).

Kowalewski and Rebow (1999) and Kowalewski and Cybulski (1998) studied the phase change of water within a cavity with the purpose of creating a benchmark solution. The velocity and temperature fields were monitored using TLC (Thermochromic Liquid Crystal) tracers and analyzed with DPIV (Digital Particle Image Velocimetry). The three-dimensional numerical model by Yeoh *et al.* (1990), based on finite differences, was used to simulate the experiment. They reported that effects such as supercooling, stagnant boundary layer at the bottom, imperfections in the ice structure, as well as non-ideal contact between ice and tray surfaces may have been responsible for the discrepancies between model and experiment.

Michałek and Kowalewski (2003) compared different models using the same reference as the previous works. In one of the models, a finite volume formulation with a fixed mesh of 145,000 volumes was adopted and the phase change was modeled by introducing an enthalpy source term in the energy equation. It was shown that the solutions agreed with each other when very fine meshes and small time steps were used. Loyola *et al.* (2019) formulated a transient finite volume model for the two-dimensional solidification based on the mass, momentum and energy conservation principles. The model was developed for a structured cartesian mesh based on the enthalpy-porosity methodology and implemented to emulate the unidirectional solidification process. The results were compared with the analytical solutions of Stefan's problem with errors close to 1% for the position of the ice and water interface for a 100 mm domain. In a similar fashion, Bourdillon *et al.* (2015) implemented finite volume models based on enthalpy-porosity using the OpenFOAM software. Differently from the previous studies, where the properties of the porous region (called mushy) were linearly distributed, Bourdillon *et al.* (2015) adopted an error function distribution. It is noteworthy that the model was also extended to consider slurry regions (ice particles suspended in the liquid medium). Tenchev *et al.* (2005) presented a convection solidification model based on finite elements. In the mesh, the connection between elements and the total number of nodes were maintained but reorganized at each time interval for the interface region. Danaila *et al.* (2014) also used an adaptive mesh finite element approach. The developed algorithm mapped the liquid/solid front and identified the interfaces between the recirculation, such as those generated by the inversion of the water density. Tests were performed at different levels of complexity and the results agreed with those of other authors.

As shown, the models that have advanced the most in recent times were those using numerical approaches, such as finite volumes or Euleurian and Lagrangian methods, which provide better accuracy at the expense of higher computational cost, even in two-dimensional simulations (Danaila *et al.*, 2014; Michałek and Kowalewski, 2003; Loyola *et al.*, 2019). This cost can be attributed to the necessity for refined meshes, the dynamics of mesh renewal at each time interval, the high nonlinearities related to the inversion of water density and the complexity of the equations to be solved. Also, the modeling of all physical phenomena associated with the solidification process, such as supercooling and the transition zone, is a burdensome task that can further increase the simulation time (Bourdillon *et al.*, 2015; Criscione *et al.*, 2015). On the other hand, Stefan-Plank's classic analytical solutions demand very low computational cost, but do not solve multidimensional problems (Carslaw and Jaeger, 1959; Crank, 1984).

Therefore, the present paper is aimed at devising a 3D model for predicting the freezing time (and the ice production rate) in ice trays. To do so, the pioneering formulation of Stefan-Planck was implemented in the domain of a single ice cube to track the position of each freezing-boundary over time. Experiments were also performed by means of a purpose-built wind-tunnel facility to gather data to proper validate the results. Also, to ensure robustness and reliability, the model was additionally verified against experimental and numerical results obtained elsewhere.

2. EXPERIMENTAL WORK

In order to validate the mathematical model, experiments were conducted in the wind-tunnel facility designed and constructed by Berno *et al.* (2019), which allows the control of the air flow rate and psychrometric conditions at the test section, which in turn emulates the door compartment of a typical domestic refrigerator, including the air supply and return ducts. To facilitate data analysis, a single volume of 57x57x44 mm and 145 ml, which is about ten times

the size of a conventional ice cube, was considered. In the experiments, the cooling curves representing the time evolution of water temperature during the phase change processes were monitored and it was possible to define the initial and final freezing points. The volume was fixed on an insulating base made of expanded polystyrene (EPS) and positioned symmetrically in relation to the air inlet duct. Concerning the z-axis, the water surface of the cube was positioned at the center of the air jet, as shown in Figure 1. Hence, most of the air flows through the top interface of the cube. The cold air flow is stagnant on the front face and drains through the side faces until it completely passes the cube. Then, the air is directed to the lower part of the test section, where the air outlet duct is located. Thus, the favored directions for cooling are the top and front surfaces. Seven thermocouples were positioned symmetrically and equally spaced as shown in Figure 2 (1 to 4 from top to bottom and 5 to 7 from front to back). In this configuration, solidification is expected to occur in a planar regime, with the preferred direction from 1 to 4 and from 5 to 7.

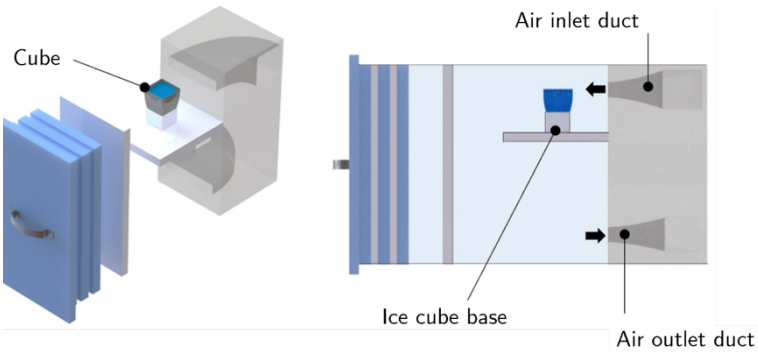

Figure 1: Ice cube positioning in the test section

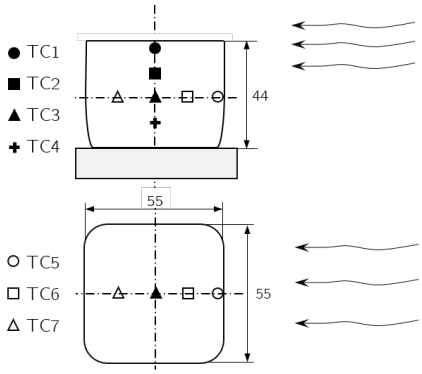

Figure 2: Thermocouple positioning in the volume

All tests were performed with air at -23 °C and a flow rate of 10 $m^3\ h^{-1}$. Three runs were performed, each one using water from different sources, such as distilled, mineral, and filtered tap water. Water was always added at 23 °C. The computation of the solidification time starts when the central thermocouple, T3, indicates 6 °C. The final solidification point could then be identified by the seven thermocouples in the volume. The effect of the solidification endpoint reading was evaluated in relation to the instrumentation placement. For this, the end of solidification was determined using the inflection point in the final stretch of the curves for each thermocouple. The inflection point at the end of the cooling curve of a finite volume always exhibits the exact moment when the latent heat liberation is ceased, i.e. solidification is complete. Thus, the total solidification time, from 6 °C to the inflection point, is shown in Table 1, while Figures 3 and 4 show the cooling curves for mineral and distilled water, respectively, where the end of the process is indicated by the red vertical lines for each of the readings. Using thermocouple T4 as a reference, representing the last solidified point, it can be observed that the highest relative deviation in the identification of the end point was 3.9%, showing that even at one extreme the inflection is identifiable. Note that the standard deviation of the differences between T4 and other readings did not exceed 1.5% compared to the total test time.

Table 1: Experimental solidification times

Parameter	Mineral water	Distilled water	Filtered tap water
Mass [g]	138	144	145
T1 [min]	189.4	196.1	194.5
T2 [min]	189.2	192.1	189.6
T3 [min]	187.1	190.3	189.1
T4 [min]	185.4	189.0	187.2
T5 [min]	188.4	191.6	190.9
T6 [min]	187.4	190.8	189.2
T7 [min]	186.1	189.9	188.8
Minimum [min]	185.4 (0.0%)	189.0 (0.0%)	187.2 (0.0%)
Maximum [min]	189.4 (2.2%)	196.1 (3.8%)	194.5 (3.9%)
Standard deviation [min]	1.5 (0.8%)	2.7 (1.4%)	2.7 (1.4%)

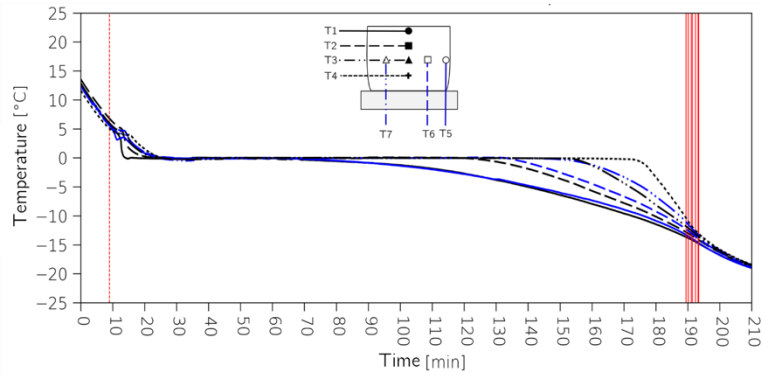

Figure 3: Test with mineral water

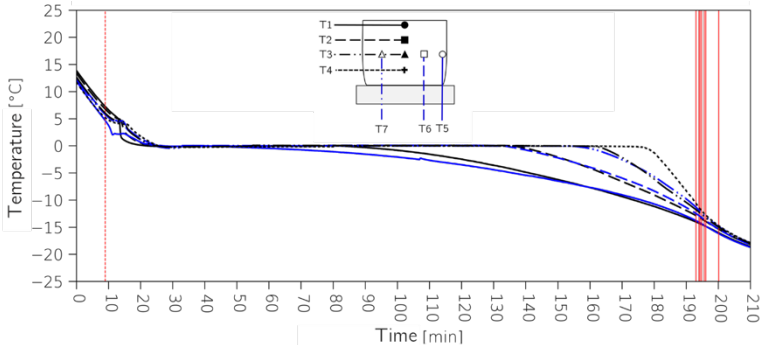

Figure 4: Test with distilled water

3. MATHEMATICAL MODELING

The proposed moving-boundary model relies on an energy balance in which the liquid center of the volume is represented by a lumped model at constant melting temperature. The heat released during freezing is conducted through the solid phase and then convectively rejected to the external medium. Stefan's formulation is the starting point and is applied to each of the domain boundaries, which in this case are the walls in contact with the ice tray and the water-air interface. As the liquid volume changes with time, the freezing front has different boundary areas $A_{i,k}$ that vary in time with respect to the outer wall areas $A_{o,k}$, as illustrated in Figure 5.

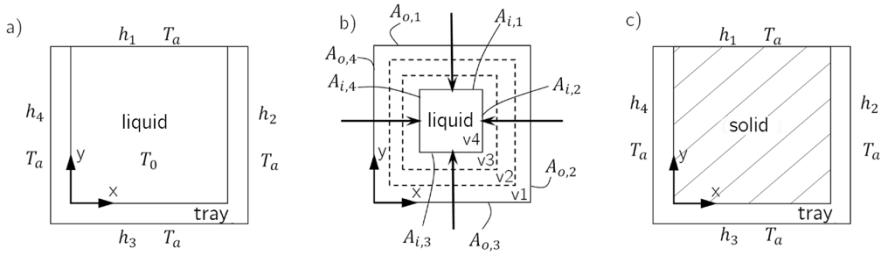

Figure 5: Moving-boundary model: (a) initial and boundary conditions, (b) process evolution, and (c) final state

Solidification occurs from the outside to the inside, such that layers of solid are added at each time step reducing the liquid volume. The model is given by the following evolutionary equation for the ice thickness, δ, which must be time-integrated for each boundary, k:

$$\frac{d\delta_k}{dt} = \frac{\Delta T}{\rho_s \lambda}\left(\frac{1}{h_k} + \frac{\delta_k}{k_s} + \frac{\delta_w}{k_w}\right)^{-1} \frac{A_{o,k}}{A_{i,k}} \tag{1}$$

being $A_{o,k}/A_{i,k}$ the ratio of the internal and external areas, re-evaluated at each time step, and ΔT the difference between the melting and surrounding temperatures. The term in parentheses is the specific resistance between the ice boundary and the outer medium, where h_k is the outer convection heat transfer coefficient for each side, δ_k is the ice thickness of each boundary, δ_w is the tray thickness, and k_s and k_w are the thermal conductivities of the ice and plastic tray, respectively. Integration with respect to time was performed using Heun's method and the boundaries advance was assumed to occur until the following stopping criterion, based on the liquid volume fraction, ϕ, was satisfied:

$$\phi = \frac{V_l}{V_l + V_s} \tag{2}$$

The real volume geometry was simplified so that the ice was inscribed in a pyramid trunk. The six required boundary conditions were obtained through a steady state simulation of the entire test section using the Star-CCM+ (2018) software, admitting an air flow rate of 10 m³ h^{-1} and a temperature of -23 °C. The boundary conditions extracted on the surface of the volume were expressed, for example, as the steady state heat flux (or heat transfer coefficient), when the water/ice is at the melting temperature, as summarized in Table 2. The resulting solidification time was of 163.2 min, starting from 0 °C to a remaining liquid volume fraction of 0.5%.

Table 2: Boundary conditions at the ice cube edges

Face	Heat transfer rate [W]	Heat flux [W m^{-2}]	h_k [W m^{-2} K^{-1}]
North	1.26	489.9	21.3
South	0.60	232.2	10.1
East	0.74	286.1	12.4
West	0.76	295.7	12.9
Top	1.18	354.2	15.4
Bottom	0.19	83.9	3.6

4. MODEL VALIDATION

In order to validate the model, its predictions were compared with the results presented in Table 1 regarding the tests with mineral, distilled and filtered tap water. In this sense, data associated with the latent period from 0 °C to the final point of solidification were considered, i.e. without considering the sensible heat transfer period. However, as the volume did not reach 0 °C in all seven thermocouple readings in a homogeneous way, for a better analysis, the comparison was made at two different extremes: (i) the beginning of the latent period is considered from the point that the first thermocouple reaches 0 °C while the others are still above 0 °C; and (ii) the latent period is considered starting from the point that all thermocouples are at 0 °C, that is, only after the last one reaches 0 °C.

In all cases, errors within a ±10% band were observed (see Table 3). The liquid and solid boundaries were also plotted over time as per Figures 7 and 8. Starting from the initial volume, each line represents the position of the solidification front in a time interval of 10 min. Note that the markers represented within the volume are aligned with the thermocouple positions during testing.

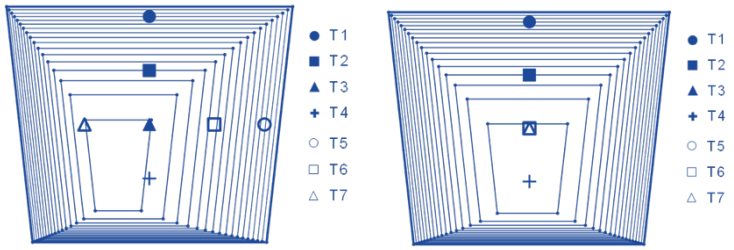

Figure 7: Solidification fronts: side view (right) and rear view (left)

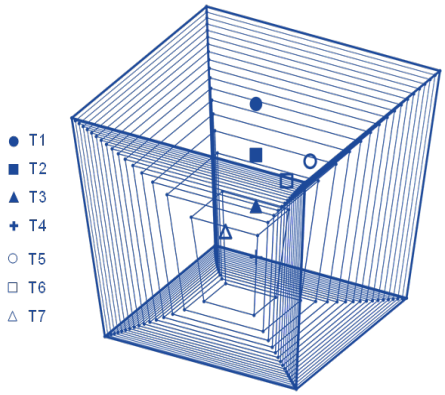

Figure 8: Solidification front: isometric view

Table 3: Mathematical model validation

	Parameter	Mineral water	Distilled water	Filtered tap water
	Exp. solidification time (T4) [min]	180.4	184.0	182.2
	Calculated solidification time [min]	163.2		
(i)	First thermocouple to reach 0 °C [min]	4.8	11.5	9.6
	Phase change time [min]	175.6	172.5	172.6
	Relative error [%]	-7.1	-5.4	-5.4
(ii)	Last thermocouple to reach 0 °C [min]	18.0	16.5	16.8
	Phase change time [min]	162.4	167.5	165.4
	Relative error [%]	0.5	-2.6	-1.3

Figure 9 shows the evolution of the solidification fronts along the cooling curves of the mineral water test, where some bands were marked for analysis. The first represents the interval in which curves T1 and T5 are no longer at 0 °C. The second does the same for thermocouples T2 and T6. In the third, T3 and T7 are explored. The last band, in turn, refers to thermocouple T4. The divergences at the end of the process are expected, since the model represents flat and not curvilinear borders, as they would be in a real case. Furthermore, at the end of the process, the air previously dissolved in the water is also concentrated in the gaseous form. Finally, the boundary conditions in the model were uniformly applied at the boundaries, whereas the tendency is for the heat transfer to be non-uniform in practice. Even so, a reasonable agreement between the solid front advancement and the temperature decay observed in thermocouples positioned symmetrically in the volume was verified.

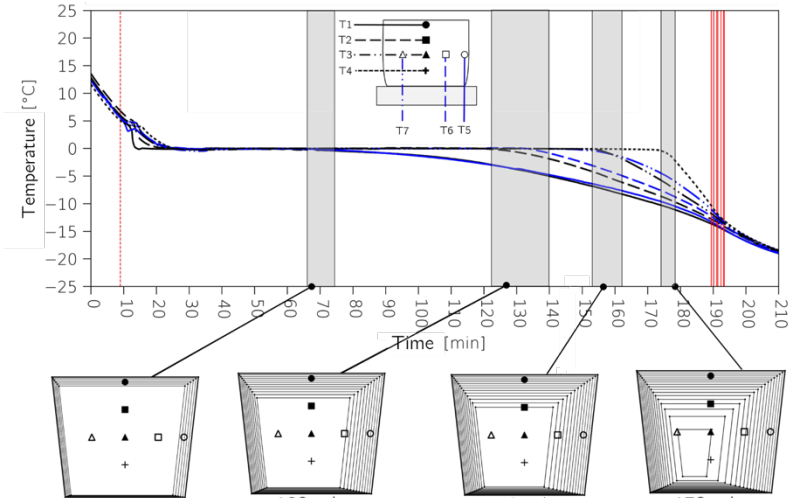

Figure 9: Evolution of the solidification fronts along the cooling curves of the mineral water test

5. FURTHER COMPARISONS

The moving-boundary model was verified against the results presented by Yeoh (1993) who, in one stage of his work, studied solidification in an open-topped square cavity though experimental observations and simulation. The experimental observation at discrete times was compared with computational predictions from its finite element model for validation purposes. Here, the same problem studied by Yeoh (1993) was simulated by the proposed moving-boundary model, so that the results were evaluated at the same discrete times.

As a boundary condition, Yeoh (1993) adopted in his simulations and experiments a constant temperature of to -10 °C for all closed walls of the cavity. The temperature at the top face, in contact with air, was predicted with an energy balance assuming a convective heat transfer coefficient of 20 W m^{-2} K^{-1} and a surrounding temperature of 20.6 °C. The only difference in relation to Yeoh's (1993) simulations is that in the proposed model, the top surface was considered adiabatic. In this way, to balance, the heat that should have entered through the top was redistributed between the other faces and was calculated considering a heat transfer coefficient of 20 W m^{-2} K^{-1} and a surrounding temperature of 20.6 °C, just like Yeoh (1993). The model was integrated with a time step of 1 s.

The experimental and numerical results of Yeoh (1993) and those obtained by the three-dimensional moving-boundary model are illustrated in Figures 10 and 11. In the cross-sectional photos, the remaining water has been removed from the cube. Then, the cube was detached from the form and cut in the transverse center plane. As expected, the ice growth occurs in a planar way and, at the end of the process, the largest concavity appears. This was seen in the two analyzed plans. Again, the more accurate model, this time with finite elements, can even predict curvature and concavities. However, the moving-boundary model predicted reasonably well the solidification front position and the remaining liquid fraction.

6. FINAL REMARKS

A three-dimensional moving-boundary model based on the Stefan (1891) solution was proposed to predict the water solidification in ice trays. The implementation was carried out for a pyramidal single volume firstly subjected to a convection boundary condition obtained from a steady-state CFD simulation with water at 0 °C. In order to validate the model and improve the analysis, experiments were conducted with an ice cube instrumented with 7 thermocouples placed in a purpose-built wind-tunnel. Concerning the experimental results, negligible differences in the solidification times were observed when feeding the tray with three different types of water: distilled, mineral and filtered. Also, the standard deviation of the differences between the reference thermocouple (T4) and other readings was lower than 1.5% in relation to the test time. Experiments showed that the inflection point at the end of the cooling curve of a finite volume always exhibits the exact moment when the latent heat liberation is ceased, i.e., solidification is complete.
Regarding model validation, errors within a ±10% band were observed for all cases when comparing simulations and experiments. Finally, the proposed model predicted reasonably well when compared to simulation and experimental

results of Yeoh (1993) from the literature with respect to the solidification front position, considering a prescribed temperature boundary condition.

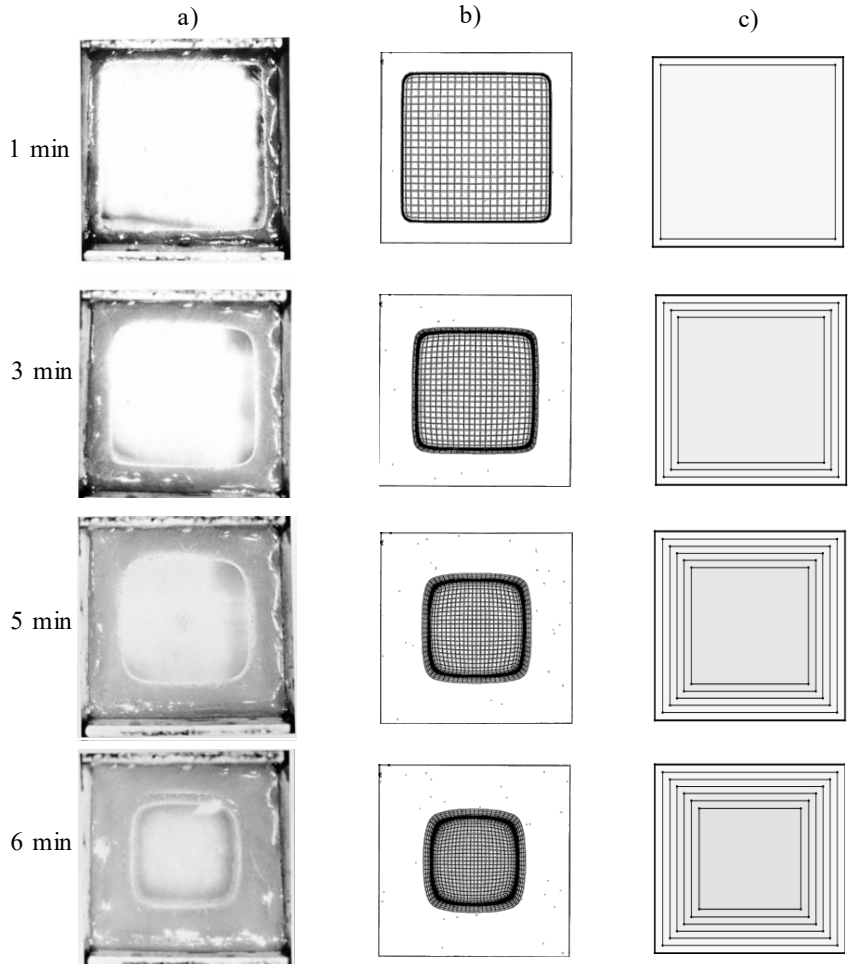

Figure 10: Top view: (a) Yeoh (1993) experiment, (b) Yeoh (1993) model and (c) proposed model

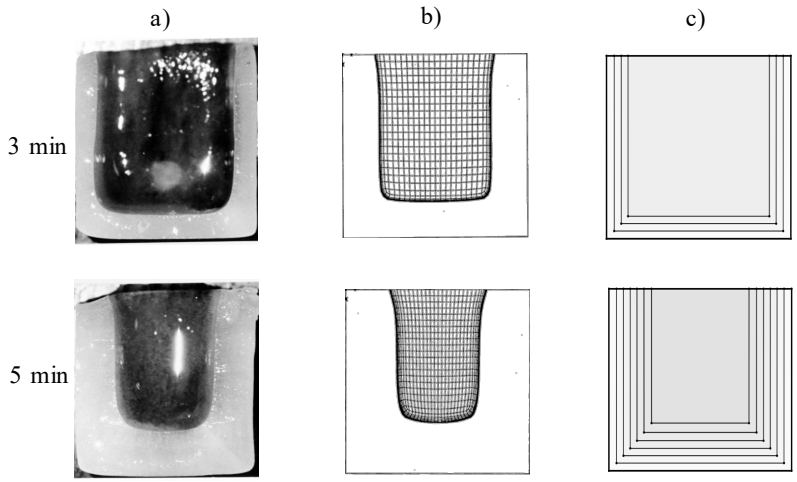

Figure 11: Cross-sectional view: (a) Yeoh (1993) experiment, (b) Yeoh (1993) model and (c) proposed model

NOMENCLATURE

Roman

A	area	(m^2)
h	convection coefficient	($W\ m^{-2}$)
k	thermal conductivity	($W\ m^{-1}\ K^{-1}$)
ρ	density	($kg\ m^3$)
T	temperature	(°C)
t	time	(s)
V	volume	(m^3)

Greek

δ	thickness	(m)
ϕ	liquid volume fraction	(dimensionless)
λ	latent of solidification	($J\ kg^{-1}$)
ρ	density	($kg\ m^3$)

Subscripts

i	inner
k	solidification front index
l	liquid
o	outer
s	ice/solid
w	plastic wall

REFERENCES

Berno, G. M., Loyola, F. R., Silva, A. C., Hermes, C. J. L. (2019). Experimental evaluation of ice production rates in ice makers of household refrigerators. 14th Congreso Iberoamericano de Ingeniería Mecánica, Cartagena, Colombia.

Bourdillon, A. C., Verdin, P. G., Thompson, C. P. (2015). Numerical simulations of water freezing processes in cavities and cylindrical enclosures. Appl. Therm. Eng., 75, 839–855.

Carslaw, H. S., Jaeger, J. C. (1959). Conduction of Heat in Solids. Oxford University Press, Oxford, UK.

Crank, J. (1984). Free and moving boundary problems. Oxford University Press, Oxford, UK.

Criscione, A., Roisman, I. V., Jakirlić, S., Tropea, C. (2015). Towards modelling of initial and final stages of supercooled water solidification. Int. J. of Therm. Sci., 92, 150–161.

Danaila, I., Moglan, R., Hecht, F., Le Masson, S. (2014). A Newton method with adaptive finite elements for solving phase-change problems with natural convection. J. Comp. Physics, 274, 826–840.

Hu, H., Argyropoulos, S. A. (1996). Mathematical modelling of solidification and melting: a review. Modell. Simul. Mater. Sci. Eng., 4(4), 371–396.

Kowalewski, T. A., Cybulski, A. (1998). Particle image velocimetry and thermometry in freezing water, Proceedings of the 8th International Symposium on flow Visualization, Sorrento, Italy.

Kowalewski, T. A., Rebow, M. (1999). Freezing of Water in a Differentially Heated Cubic Cavity. International J. Comp. Fluid Dynamics, 11(3-4), 193–210.

Loyola, F. R., Barboza, L. Z., Hermes, C. J. L. (2019). Numerical simulation of water solidification in square ice trays: A simplified enthalpic formulation. Proceedings of the 25th IIR International Congress of Refrigeration, Montreal, Canada.

Meier, A., Martinez, M. (1996). Energy Use of Ice Making in Domestic Refrigerators. ASHRAE Trans., 102(2), 1071–1076.

Michałek, T., Kowalewski, T. A. (2003). Simulations of the Water Freezing Process – Numerical Benchmarks. Task Quarterly, 7(3), 389–408.

Morgan, K. (1981). A numerical analysis of freezing and melting with convection. Comput. Methods in Appl. Mechanics and Eng., 28(3), 275–284.

Plank, R. (1913). Die Gefrierdauer von Eisblocken. Zeitschrift für die gesamte Kalte-industrie, 20(6), 109–114.

Plank, R. (1941). Beiträge zur Berechnung und Bewertung der Gefriergeschwindigkeit von Lebensmitteln. Zeitschrift für die gesamte Kälte-Industrie: Beihefte, 48(10).

Star-CCM+. (2018). Star-CCM+ user guide version 13.04. Siemens PLM Software.

Stefan, J. (1891). Ueber die Theorie der Eisbildung, insbesondere über dieEisbildung im Polarmeere. Annalen der Physik, 278(2), 269–286.

Tenchev, R. T., Mackenzie, J. A., Scanlon, T. J., Stickland, M. T. (2005). Finite element moving mesh analysis of phase change problems with natural convection. Int. J. Heat Fluid Flow, 26(4), 597–612.

Voller, V. R., Prakash, C. (1987). A fixed grid numerical modelling methodology for convection-diffusion mushy region phase-change problems. Int. J. of Heat Mass Transfer, 30(8), 1709–1719.

Voller, V. R., Swaminathan, C. R., Thomas, B. G. (1990). Fixed grid techniques for phase change problems: A review. Int. J. for Numer. Methods in Engineering, 30(4), 875–898.

Yashar, D. A. (2012). Development of a Method to Measure the Energy Consumption of Automatic Icemakers in Domestic Refrigerators with Single Speed Compressors. Revision 1, NIST Technical Note 1759, NIST Gaithersburg, MD, USA.

Yashar, D. A., Park, K. -J. (2011). Energy Consumption of Automatic Ice Makers Installed in Domestic Refrigerators. NIST Technical Note 1697, Gaithersburg, MD, USA.

Yeoh, G. H. (1993). Natural Convection in a Solidifying Liquid. Ph.D. Thesis, The University of New South Wales, Sydney, Australia.

ACKNOWLEDGEMENTS

The authors appreciate the support from Whirlpool and Embrapii through Grant No. PPOL-1710.0012. Additional funding was provided by the National Institutes of Science and Technology Program (CNPq Grant No. 404023/2019-3; FAPESC Grant No. 2019TR0846).